Long period gratings in air-core photonic bandgap fibers

Yiping Wang, Wei Jin, Jian Ju, Haifeng Xuan, Hoi Lut Ho, Limin Xiao, and Dongning Wang

Department of Electrical Engineering, The Hong Kong Polytechnic University, Hung Hom, Kowloon, Hong Kong
eewjin@polyu.edu.hk, ypwang@china.com

Abstract: Long period fiber gratings in hollow-core air-silica photonic bandgap fibers were produced by use of high frequency, short duration, CO_2 laser pulses to periodically modify the size, shape and distribution of air holes in the microstructured cladding. The resonant wavelength of these gratings is highly sensitivity to strain but insensitive to temperature, bend and external refractive index. These gratings can be used as stable spectral filters and novel sensors.

OCIS codes: (060.2310) Fiber optics; (050.2770) Gratings; (060.0060) Fiber optics and optical communications

References and links

1. R. F. Cregan, B. J. Mangan, J. C. Knight, T. A. Birks, P. S. Russell, P. J. Roberts, and D. C. Allan, "Single-mode photonic band gap guidance of light in air," Science **285**, 1537-1539 (1999).
2. J. C. Knight, "Photonic Crystal Fibers," Nature 424, 847-851 (2003).
3. C. M. Smith, N. Venkataraman, M. T. Gallagher, D. Muller, J. A. West, N. F. Borrelli, D. C. Allan, and K. W. Koch, "Low-loss hollow-core silica/air photonic bandgap fibre," Nature **424**, 657-659 (2003).
4. B. J. Mangan, L. Farr, A. Langford, P. J. Roberts, D. P. Williams, F. Couny, M. Lawman, M. Mason, S. Coupland, R. Flea, and H. Sabert, "Low-loss (1.7dB/km) hollow-core photonic bandgap fiber," in proceeding of OFC 2004, paper PDF24, Los Angeles, USA (2004).
5. P. J. Roberts, F. Couny, H. Sabert, B. J. Mangan, D. P. Williams, L. Farr, M. W. Mason, A. Tomlinson, T. A. Birks, J. C. Knight, and P. S. J. Russell, "Ultimate low loss of hollow-core photonic crystal fibres," Opt. Express **13**, 236-244 (2005).
6. D. G. Ouzounov, F. R. Ahmad, D. Müller, N. Venkataraman, M. T. Gallagher, M. G. Thomas, J. Silcox, K. W. Koch, and A. L. Gaeta, "Generation of megawatt optical solitons in hollow-core photonic band-gap fibers " Science **301**, 1702-1704 (2003).
7. G. Humbert, J. C. Knight, G. Bouwmans, P. S. Russell, D. P. Williams, P. J. Roberts, and B. J. Mangan, "Hollow core photonic crystal fibers for beam delivery," Opt. Express **12**, 1477-1484 (2004).
8. J. M. Fini, "Microstructure fibres for optical sensing in gases and liquids," Meas. Sci. Technol. **15**, 1120-1128 (2004).
9. Y. L. Hoo, W. Jin, H. L. Ho, J. Ju, and D. N. Wang, "Gas diffusion measurement using hollow-core photonic bandgap fiber," Sens. Actuators B **105**, 183-186 (2005).
10. F. Benabid, J. C. Knight, G. Antonopoulos, and P. S. J. Russell, "Stimulated raman scattering in hydrogen-filled hollow-core photonic crystal fiber," Science **298**, 399-402 (2002).
11. V. Bhatia and A. M. Vengsarkar, "Optical fiber long-period grating sensors," Opt. Lett. **21**, 692-694 (1996).
12. Y. P. Wang, D. N. Wang, W. Jin, Y. J. Rao, and G. D. Peng, "Asymmetric long period fiber gratings fabricated by use of CO_2 laser to carve periodic grooves on the optical fiber," Appl. Phys. Lett. **89**, 151105 (2006).
13. B. J. Eggleton, P. S. Westbrook, R. S. Windeler, S. Spalter, and T. A. Strasser, "Grating resonances in air-silica microstructured optical fibers," Opt. Lett. **24**, 1460-1462 (1999).
14. Y. P. Wang, L. M. Xiao, D. N. Wang, and W. Jin, "Highly sensitive long-period fiber-grating strain sensor with low temperature sensitivity," Opt. Lett. **31**, 3414-3416 (2006).
15. K. Morishita and Y. Miyake, "Fabrication and resonance wavelengths of long-period gratings written in a pure-silica photonic crystal fiber by the glass structure change," J. Lightwave Technol. **22**, 625-630 (2004).
16. J. H. Lim, K. S. Lee, J. C. Kim, and B. H. Lee, "Tunable fiber gratings fabricated in photonic crystal fiber by use of mechanical pressure," Opt. Lett. **29**, 331-333 (2004).
17. P. Steinvurzel, E. D. Moore, E. C. Magi, B. T. Kuhlmey, and B. J. Eggleton, "Long period grating resonances in photonic bandgap fiber," Opt Express **14**, 3007-3014 (2006).
18. http://www.crystal-fibre.com.

#91088 - $15.00 USD Received 20 Dec 2007; revised 11 Feb 2008; accepted 11 Feb 2008; published 13 Feb 2008

19. B. H. Kim, Y. Park, T. J. Ahn, D. Y. Kim, B. H. Lee, Y. Chung, U. C. Paek, and W. T. Han, "Residual stress relaxation in the core of optical fiber by CO_2 laser irradiation," Opt Lett. **26**, 1657-1659 (2001).
20. J. A. West, C. M. Smith, N. F. Borrelli, D. C. Allan, and K. W. Koch, "Surface modes in air-core photonic band-gap fibers," Opt. Express **12**, 1485-1496 (2004).
21. H. K. Kim, M. Digonnet, G. Kino, J. Shin, and S. Fan, "Simulation of the effect of the core ring on surface and air-core modes in photonic bandgap fibers," Opt. Express **12**, 3436-3442 (2004).
22. G. Bouwmans, F. Luan, J. C. Knight, P. S. J. Russell, L. Farr, B. J. Mangan, and H. Sabert, "Properties of a hollow-core photonic bandgap fiber at 850 nm wavelength," Opt. Express **11**, 1613-1620 (2003).
23. J. Ju, W. Jin, and M. S. Demokan, "Two-mode operation in highly birefringent photonic crystal fiber," IEEE Photon. Technol. Lett. **16**, 2472-2474 (2004).
24. B. L. Bachim and T. K. Gaylord, "Polarization-dependent loss and birefringence in long-period fiber gratings," Appl. Opt. **42**, 6816-6823 (2003).
25. D. Lee, Y. Jung, Y. S. Jeong, K. Oh, J. Kobelke, K. Schuster, and J. Kirchof, " Highly polarization-dependent periodic coupling in mechanically induced long period grating over air-silica fibers," Opt. Lett. **31**, 296-298 (2006).
26. Y. J. Rao, Y. P. Wang, Z. L. Ran, and T. Zhu, "Novel fiber-optic sensors based on long-period fiber gratings written by high-frequency CO_2 laser pulses," J. Lightwave Technol. **21**, 1320-1327 (2003).
27. H. J. Patrick, C. C. Chang, and S. T. Vohra, "Long period fibre gratings for structural bend sensing," Electron. Lett. **34**, 1773-1775 (1998).
28. Y. P. Wang and Y. J. Rao, "A novel long period fiber grating sensor measuring curvature and determining bend-direction simultaneously," IEEE Sensors Journal **5**, 839-843 (2005).

1. Introduction

Since the first demonstration of light guiding in an air-core photonic bandgap fiber (PBF) [1], tremendous progress has been made in the understanding, design and fabrication of such fibers [2-4]. Practical PBFs with loss as low as 1.2dB/km has been reported [5]. The guiding of light in air has a number of advantages such as lower Rayleigh scattering, reduced nonlinearity, increased damaging threshold, novel dispersion characteristics and potentially lower loss compared to conventional optical fibers. These properties are likely to have a lasting effect on optical signal transmission, high power laser pulse delivery and shaping, etc. [6-7]. The hollow-core characteristic of the PBFs also allow strong light/material interaction inside the fiber-core over an extended length, which offers a new platform for developing ultra-sensitive and distributed gas and liquid sensors [8-9] and for studying nonlinear optics for gases [10]. To increase the impact of the technology, in-fiber components such as wavelength/polarization selective filters are required for manipulating light of different wavelengths/polarizations. Such components have been well developed for conventional glass fiber technology but are not yet available in the format of hollow-core PBFs. We report here long period fiber grating (LPFGs) filters made by periodically modify the cladding holes of an air-core PBF.

LPFGs have been made in conventional single mode fibers (SMFs) [11-12], index-guiding photonic crystal fibers (IG PCFs) [13-16] as well as solid-core PBFs made by filling high index fluid into the holes of IG PCFs [17]. The principal mechanisms for the LPFG formation in such solid core fibers are refractive index variation of core (sometimes also cladding) material through UV photo-sensitivity, external applied stress, residual stress-relaxation and/or glass structural change [11-17]. However, so far no report on gratings formed in air-core PBFs, probably due to the difficulty in introducing refractive index modulation into air-holes in which over 95% light energy of the fundamental mode is located. In the following sections we describe the process for fabricating LPFGs in air-core PBFs, discuss the possible mechanism of grating formation and study the response of these LPFGs to strain, temperature, bend and external refractive index.

2. Fabrication of LPFGs

An experimental setup similar to that in [12] was used to fabricate LPFGs in hollow-core PBFs. A pulsed CO_2 laser is used to modify the micro-structures along the fiber, and an Er-doped ASE source and an optical spectrum analyzer (OSA) are employed to observe the evolution of transmitted spectrum during LPFG fabrication process. The fiber samples used here are Crystal-Fiber's HC-1500-02 PBFs [18] with a cross-section shown in Fig. 1(a). The

#91088 - $15.00 USD Received 20 Dec 2007; revised 11 Feb 2008; accepted 11 Feb 2008; published 13 Feb 2008

PBFs are spliced to Corning SMF-28 fibers at both ends for connections to the ASE source and the OSA. The CO_2 laser emits pulses with a width of 2.2μs, a repetition rate of 10kHz and an average power of ~ 0.2W. The CO_2 laser beam was focused to a spot of ~ 35μm in diameter and the PBF was placed on the focal plane of the beam. The CO_2 beam is scanned, via a computer controlled two-dimensional optical scanner, transversely across the PBF to make a grating notch. The line speed of scanning is 2.9mm/s, the accumulated time for laser pulses to hit a particular point on the fiber surface is estimated to be 265.6μs. These high-frequency, short duration, CO_2 laser pluses hit repeatedly on one side of the PBF and induce a local high temperature, causing ablation of glass on the surface and change of shapes, sizes, locations, and even complete collapse of some of the air holes in the cladding [Fig. 1(b)]. This results in a notch being created on the surface of the fiber [Fig. 1(c)]. The laser beam is then moved longitudinally along the fiber by a grating pitch Λ and the same process is repeated to create the 2nd, 3rd, and Nth notches. An LPFG with N notches or N periods is then produced. This process of making N notches is called one scanning cycle. The notch depth can be increased by having more scanning cycles. As a result, periodic notches with required depths are created along the fiber surface. Fig. 1(c) show the periodic notches created on a PBF after 50 scanning cycles. The cross section, as shown in Fig. 1(b), of the PBF at the notched region is asymmetric due to the collapse of air holes and the ablation of glass on one side of the fiber. The outer rings of air holes in the cladding, facing to the CO_2 laser irradiation, were largely deformed; however, little or no deformation were observed in the innermost ring of air-holes and in the hollow core. The width and depth of the notches are ~60μm and ~15μm, respectively.

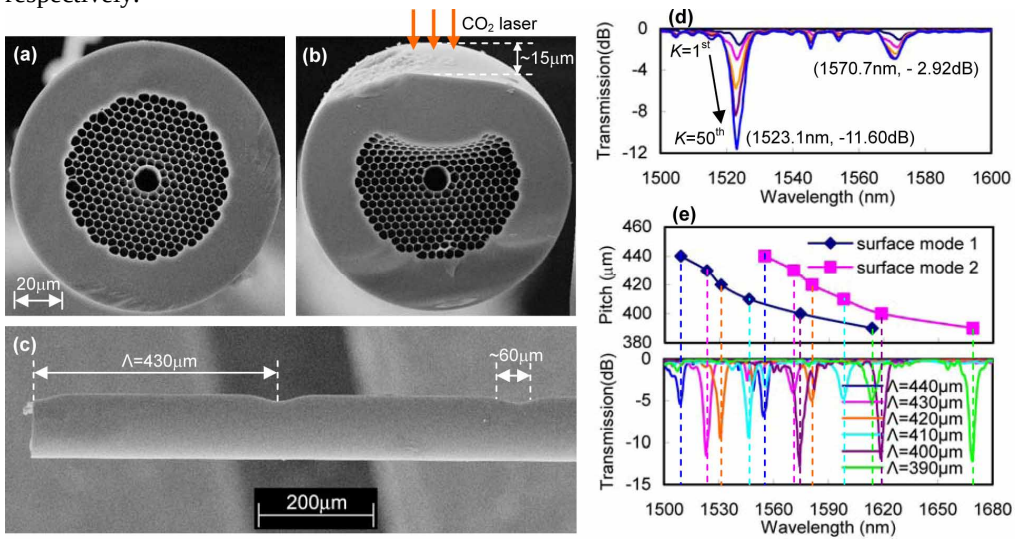

Fig. 1. Scanning electron micrographs of PBF cross-sections (a) before and (b) after CO_2 laser irradiation. (c) Periodic notches on PBF after 50 scanning cycles. (d) Evolution of the transmitted spectrum of LPFG with 40 periods and a grating pitch of 430μm with increasing number of scanning cycles (K=1st , 2nd , …50th). (e) Variation of LPFG resonant wavelengths with grating pitch (upper panel) and their transmission spectrums (lower panel). These LPFGs have 40 periods and were written at a position 5 to15cm away form the output end of 2m PBF. The PBF is pigtailed at both ends with SMF28 fibers. All transmission spectra were measured with an OSA with a resolution of 1nm.

Figure 1(d) shows the measured transmitted spectrum of a 40-period LPFG made by the above process. The 3dB-bandwidth is ~5.6nm, which is much narrower than that of the LPFGs with same number of grating periods in conventional SMFs [11-12] and in IG PCFs [13-16] and can be further narrowed down by increasing the number of grating periods. The insertion loss of the LPFG is very low (<0.3dB), because most light is guided in the hollow-core where no deformation was observed. A proper choice of the fabrication parameters is

#91088 - $15.00 USD Received 20 Dec 2007; revised 11 Feb 2008; accepted 11 Feb 2008; published 13 Feb 2008

critical for the fabrication of such a high-quality LPFG. High energy pulses with a long irradiation time may cause large deformation or collapsing of the holes and thus a higher insertion loss, while low energy pulses with short irradiation time maybe insufficient to inscribe an LPFG on the PBF. The LPFG writing process is quite repeatable in terms of resonant wavelength but the depth of the resonance shows some variations for the same number of scanning cycles. This is because that the CO_2 laser power fluctuates up to ±10% over a period of several minutes and a laser with better stability would overcome this problem.

3. Mechanism of LPFG formation

Periodic perturbations along the axis of fiber are required to achieve resonant mode coupling in an LPFG. For the LPFG shown in Fig. 1(d), the required periodic perturbations could be due to two factors: the stress relaxation induced refractive index perturbation of glass material and the changes in air-hole sizes, shapes and locations that perturb the waveguide (geometric) structure. Residual stress exists in glass after a preform comprising of stacked capillaries was drawn to a PBF. The irradiation of CO_2 laser beam on the fiber induces localized high temperature and relaxes the residual stress around the notched region, resulting in refractive index perturbation of glass due to the photo elastic effect [12, 19]. However, as most light power of the fundamental mode (>95%) is in the air region [18], the effect of stress relaxation on the mode index is expected to be much smaller than that for conventional fibers and solid core PCFs. On the other hand, as shown in Fig. 1(b), the collapse of air-holes in the cladding results in a change in the shapes, sizes and locations of air-holes, which change the air-filling fractions and the waveguide structure and perturbs the mode fields and effective indexes of the core, surface and cladding modes. There could also be weak deformation of the hollow-core, although it is not observable in our experiments. We believe that the periodic perturbation of the waveguide (geometric) structure is the dominant factor that causes resonant mode coupling, although the stress relaxation-induced index variation may also contribute a little. The observed resonances in Fig. 1(d) could be due to coupling of the fundamental mode to leaky higher order (core or surface-like) modes that are directly lost; however, as the core and the surface-like modes are guided modes that are confined by the holey photonic crystal cladding, it seems unlikely that these modes are lost over a short length (5 to 15cm) of fiber and to induce significant loss dips in the transmitted spectrum. Alternatively a two-step coupling process might be involved: light satisfying the phase matching condition is coupled from the core mode to higher order core or surface-like modes due to the spatial overlap of these modes at the perturbed region, and then to quasi-continuum of extended modes and eventually lost. This process may be regarded as similar to the loss mechanism of PBFs at an anti-crossing point [3, 20, 21], however, we here are working in a wavelength range away from the anti-crossing points and phase matching is not satisfied under normal conditions but is achieved through a periodic perturbation of the waveguide structure, i.e., a LPFG in the fiber. Further investigation is needed to understand the exact coupling process involved.

To investigate the phase matching condition as function of wavelength, six LPFGs with different pitches and the same number of grating periods were written in the PBF. The measured resonant wavelength as functions of the grating pitch is shown in Fig. 1(e), the resonant wavelength decreases with the increase in grating pitch, which is opposite to the LPFGs in the conventional SMFs [11-12]. For each of the LPFGs, two attenuation pits, as shown in Fig. 1(e), were observed within 1500 to 1680nm, indicating that the fundamental mode is coupled to two different higher order (core or surface-like) modes.

We studied in detail the mode coupling in the LPFG by cutting the PBF at various notches and recording the near field images by use of a microscope with its eyepiece lens replaced by an infrared camera. A wavelength tunable laser was used as the light source to illuminate the PBF via a lead-in SMF-28 fiber and some of the recorded images are shown in Fig. 2. Before the LPFG was created, the light intensity is mainly in the fundamental mode [Fig. 2(a)]. With an increase in the number of grating pitches, for the input light at resonant wavelength of 1523.1nm, light energies near the core-cladding interface and in the holey cladding region are

#91088 - $15.00 USD Received 20 Dec 2007; revised 11 Feb 2008; accepted 11 Feb 2008; published 13 Feb 2008

gradually enhanced whereas that in the fundamental mode is reduced, as can be seen from Figs. 2(b) and 2(c). At the 19th notch, most energy in the fundamental mode is coupled out so that the light energies near the core-cladding interface and in the holey region were clearly observed and light intensity at the center of hollow core becomes very weak. Light coupled into the cladding region is mainly distributed within the holey cladding region as outlined by the dashed curve, and the energy in the side facing to CO_2 laser irradiation is stronger than that in the opposite side. The near field images with weak intensity at the core center are believed to be the second order core modes (TE01, TM01 and HE21), these modes can not be seen in the present of strong fundamental mode, but become apparent with the reduction of fundamental mode intensity. Away from the resonant wavelength, e.g. at 1540.0nm [Fig. 2(d)], light power is mainly in the fundamental mode inside the hollow-core and no clear cladding mode was observed.

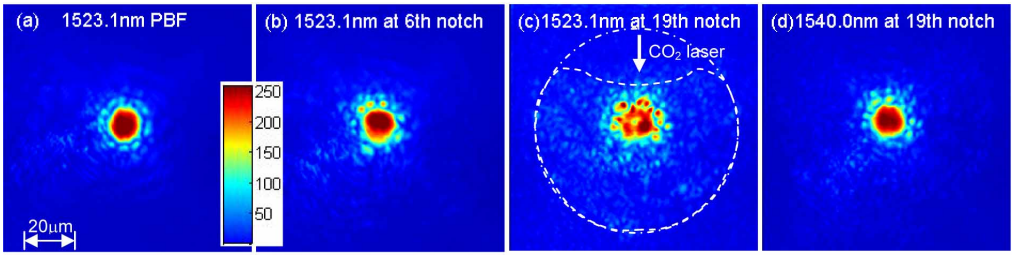

Fig. 2. (a). Near field image in a PBF without LPFG. (b) Near field images of an LPFG at the resonant wavelength of 1523.1nm when the LPFG was cut at 6th notch. (c) Near field images of the same LPFG observed at the 19th notch at 1523.1nm. (d) Near field images observed at the 19th notch when the light wavelength was tuned to 1540.0nm. The transmitted spectrum of the LPFG is illustrated in Fig. 1(d). The dot-dashed circle and the dashed curve in (c) outline the cross-sections, as illustrated in Figs. 1(a) and 1(b), of air-hole region before and after the CO_2 laser irradiation, respectively.

The existence of the second order core modes was further verified through the study of another sample comprising a 1.1m HC-1550-2 PBF pigtailed at both ends by SMF28 fibers. Figure 3(a) shows the spectrums recorded with an OSA with a resolution of 0.01nm. Background oscillations or ripples are observed in transmitted spectrums of the PBF, either with or without an LPFG. The ripples appearing in both spectrums have the same period and are obviously due to modal interference as no polarizing element was inserted into the system. This observation agrees with the findings by others in which the HC-1550-2 fiber, although it is designed to be single mode, actually supports both the fundamental and the second order modes [3, 20]. The ripples' amplitude in dB [black and pink traces in Fig. 3(a)] becomes bigger after the LPFG was written, this is because, without the LPFG, the power in the second order modes is much lower than in the fundamental mode and the interference fringe contrast in dB is low; the LPFG resonantly couples out the power in the fundamental mode and reduces it to a level similar to that of the second order modes, which increases the fringe contrast in the dB scale. The ripples amplitude in a linear scale (blue and red traces in Fig. 3(a)), which represents that absolute value of the fringe amplitude, is actually bigger without the LPFG. The ripples are amplitude-modulated as can be seen clearly in the "pink" spectrum in Fig. 3(a). This is because the PBF is birefringent due to unintentional deformation in the drawing process [22] and the superposition of two sets of interference fringes; each corresponds to a different polarization state and has a different period, results in an amplitude-modulated beating signal [23].

Figures 3(b), 3(c), and 3(d) illustrates far field images of the LPFG when the input light wavelength was tuned to around points labeled as 'b', 'c' and 'd', respectively, in the oval-insert in Fig. 3(a). These images were observed via a system comprising of a tunable laser and an infrared camera. The PBF was cut near the lead-out SMF28 fiber and at a distance of ~5mm away from the LPFG. The length of the PBF with LPFG is then slightly shorter than the original pigtailed samples and is ~1m. It can be seen from Fig. 3(a) that the intensity

#91088 - $15.00 USD Received 20 Dec 2007; revised 11 Feb 2008; accepted 11 Feb 2008; published 13 Feb 2008

transmitted through the PBF is periodically modulated as approximately sinusoidal function of wavelength due to the mode interference. The relative intensities of the "lobes" shown in Figs. 3(b), 3(c), and 3(d) actually vary alternatively when the wavelength was tuned and we only recorded those images where the two lobes have similar intensities, which occurred only once within each period. The images shown in Figs. 3(b), 3(c) and 3(d) are the typical two mode interference patterns [23]. When the wavelength is tuned far from the resonant wavelength, e.g., at 1640.92nm, as shown in Fig. 3(e), the observed far field image is the familiar fundamental mode pattern as the power of the second order modes is significantly lower than the fundamental mode.

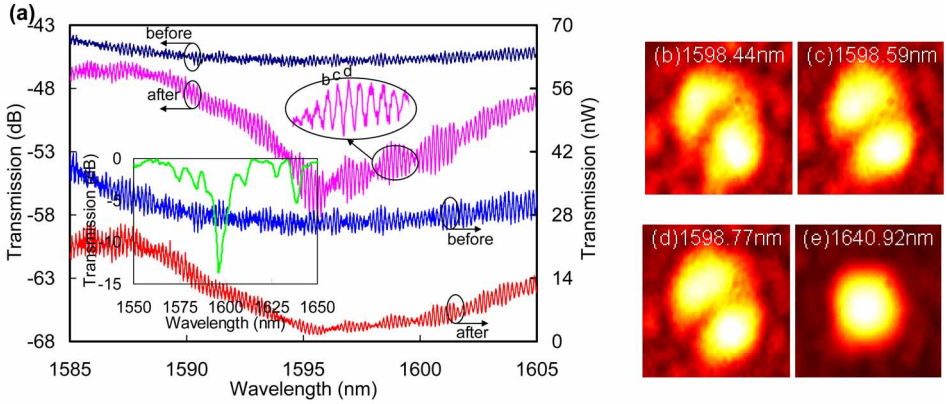

Fig. 3. (a). Transmitted spectrums of 1.1m PBF before (black and blue) and after (pink and red) an LPFG with a grating pitch of 395μm and 20 grating periods was created. The spectrums were observed with an OSA with a resolution of 0.01nm. The left (for black and pink traces) and right (for blue and red traces) axes are in the logarithmic and linear scales, respectively. The PBF is pigtailed with SMF28 fibers in both ends and the LPFG was written near the output end of the PBF. The square-insert (the green trace) shows the LPFG's transmitted spectrum measured with a 1nm resolution, and the resonant wavelength is 1595.8nm. (b), (c), and (d) Far field images at the output of the LPFG at the wavelengths around the points labeled as 'b', 'c' and 'd' in the oval-insert in (a). The pigtail at the output end was cut to observe these images.

4. Characterization of LPFGs

The polarization dependent losses (PDLs) of the PBF sample in Fig. 3, with and without the LPFG, were measured by the Agilent 81910A photonic all-parameter analyzer. As shown in Fig. 4(a), the PDL of the PBF without LPFG is 0.6±0.5dB and is increased to as high as 25dB around the resonant wavelength after an LPFG was written. This is much larger than that of the CO_2-laser-induced LPFGs in conventional SMFs (~1.2dB) [24]. The large PDL is believed to be due to the significant asymmetry in waveguide cross-section [Fig. 1(b)] caused by the changes and collapses of air holes, which induces large birefringence and asymmetrical mode field profile. Strong PDLs were also observed in mechanically induced LPGs on hollow fibers with a ring core, and hexagonal- and circular-boundary holey fibers [25].

The responses of the LPFG in the air-core PBF to strain, temperature, bend and external refractive index are also investigated. The temperature sensitivity of the resonant wavelength and the peak transmission attenuation are respectively ~2.9pm/°C and -0.0051dB/°C [Fig. 4(b)]. The wavelength sensitivity is one to two orders of magnitude less than those of the LPFGs in the conventional SMFs [11, 26]. When the curvature of LPFG was increased to 13.3m^{-1}, the resonant wavelength and the peak transmission attenuation changed by only ±8pm and 0.71dB [Fig. 4(c)], respectively. The wavelength sensitivity to bend is three to four orders of magnitude less than those of the LPFGs in the conventional SMFs [27, 28]. In addition, when the LPFG in the PBF was immerged into the refractive index liquids (from Cargill Labs) with indexes of 1.40, 1.45 and 1.50, respectively, the resonant wavelength and peak transmission attenuation hardly changed, whereas the LPFGs in the conventional SMFs are very sensitive to external refractive index, especially when the index is about 1.45 [11].

#91088 - $15.00 USD Received 20 Dec 2007; revised 11 Feb 2008; accepted 11 Feb 2008; published 13 Feb 2008

These stable optical features are advantage to their applications in the optical devices and sensors. With the increase of applied tensile strain, the resonant wavelength of our LPFG shifted linearly toward shorter wavelength with a strain sensitivity of -0.83nm/mε and the peak transmission attenuation was decreased with a sensitivity of 2.03dB/mε [Fig. 4(d)]. The wavelength sensitivity to strain is two times higher than that of LPFGs in conventional SMFs [11, 26], indicating that our LPFG may be used as a strain sensor without cross-sensitivity to temperature, curvature, and external refractive index.

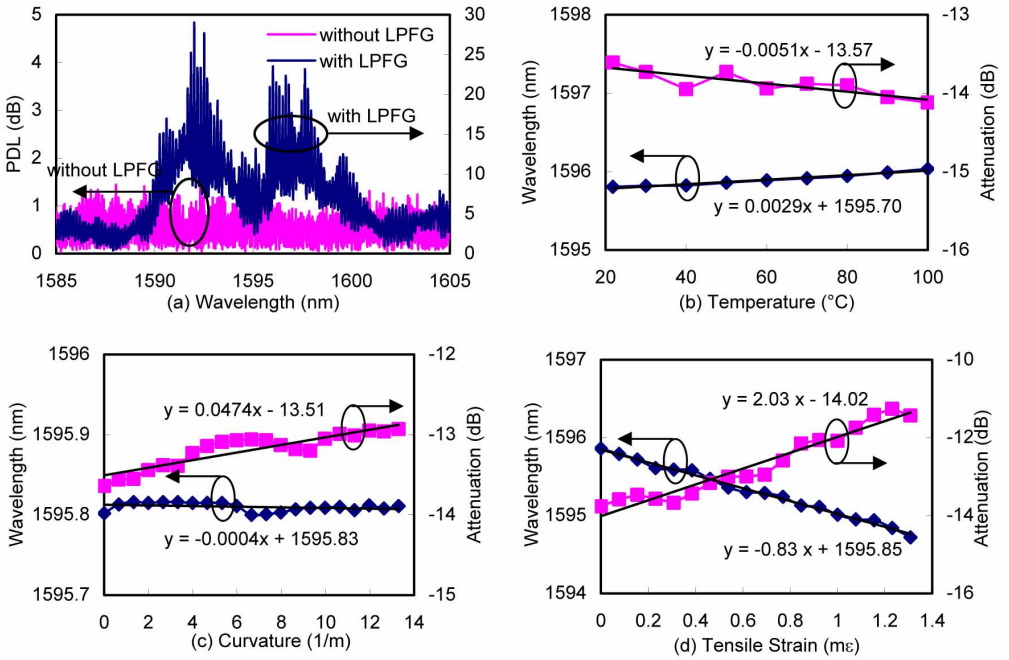

Fig. 4. (a). PDL of PBF with and without an LPFG. The LPFG sample is the same as in Fig. 3. Measured resonant wavelength and peak transmitted attenuation of the LPFG as functions of temperature (b), curvature (c), and tensile strain (d).

5. Conclusion

High-quality LPFGs were produced in air-core PBFs by use of high frequency short duration CO_2 laser pulses to periodically vary the size, shape and location of the air-holes in the holey cladding. The variation of cladding holes changes mainly the waveguide structure, instead of the refractive index of the materials forming the waveguide. This is different from LPFGs inscribed in solid core fibers in which the main perturbation is on the refractive index of the materials forming the fiber. Although the mechanism for resonant mode coupling is not well understood yet and further investigation is needed, we suspect that a two-step process could be involved: the fundamental core mode is coupled to discrete higher order (core or surface-like) modes and then to lossy quasi-continuum of cladding and radiating modes. The LPFGs in hollow-core PBFs have unique properties such as very large PDL, very small sensitivity or insensitivity to temperature, bend and external refractive index, and large strain sensitivity. These novel LPFGs will find applications in both optical devices and sensors.

Acknowledgment

The work was supported by Hong Kong SAR government through a CERG grant PolyU5182/ 07E.

#91088 - $15.00 USD Received 20 Dec 2007; revised 11 Feb 2008; accepted 11 Feb 2008; published 13 Feb 2008